J Electr Eng Technol Vol. 8, No. 5: 1021-1028, 2013
http://dx.doi.org/10.5370/JEET.2013.8.5.1021

ISSN(Print) 1975-0102
ISSN(Online) 2093-7423

Rotor Speed-based Droop of a Wind Generator in a Wind Power Plant for the Virtual Inertial Control

Jinsik Lee*, Jinho Kim*, Yeon-Hee Kim*, Yeong-Han Chun, Sang Ho Lee***, Jul-Ki Seok§ and Yong Cheol Kang†**

Abstract – The frequency of a power system should be kept within limits to produce high-quality electricity. For a power system with a high penetration of wind generators (WGs), difficulties might arise in maintaining the frequency, because modern variable speed WGs operate based on the maximum power point tracking control scheme. On the other hand, the wind speed that arrives at a downstream WG is decreased after having passed one WG due to the wake effect. The rotor speed of each WG may be different from others. This paper proposes an algorithm for assigning the droop of each WG in a wind power plant (WPP) based on the rotor speed for the virtual inertial control considering the wake effect. It assumes that each WG in the WPP has two auxiliary loops for the virtual inertial control, i.e. the frequency deviation loop and the rate of change of frequency (ROCOF) loop. To release more kinetic energy, the proposed algorithm assigns the droop of each WG, which is the gain of the frequency deviation loop, depending on the rotor speed of each WG, while the gains for the ROCOF loop of all WGs are set to be equal. The performance of the algorithm is investigated for a model system with five synchronous generators and a WPP, which consists of 15 doubly-fed induction generators, by varying the wind direction as well as the wind speed. The results clearly indicate that the algorithm successfully reduces the frequency nadir as a WG with high wind speed releases more kinetic energy for the virtual inertial control. The algorithm might help maximize the contribution of the WPP to the frequency support.

Keywords: Virtual inertial control, Rotor speed-based droop, Wind power plant control, Frequency support and Wake effect.

1. Introduction

A power system frequency should be maintained within the allowed limits to supply high-quality electricity. If a large disturbance such as a generator outage or a load increase occurs in the system, the frequency declines. Without proper action, the frequency keeps decreasing and consequently the power system might collapse. To avoid it, as soon as the system frequency drops, the synchronous generators (SGs) inherently release the kinetic energy stored in the rotating masses of the SGs to the system and this inertial response prevents the frequency from falling. Simultaneously, the SGs, which have the spinning reserve, activate the primary control by supplying the active power proportional to the frequency deviation based on the droop characteristics. After the primary control, the secondary and tertiary controls are activated successively by the system operator to recover the frequency to the nominal value [1].

On the other hand, due to the technical advances and economic viability over the last decades, a large number of wind generators (WGs) have been integrated into power systems. The global installed wind generation capacity had increased to 238 GW as of 2011 and is expected to increase to 832 GW by 2020 [2]. Korea started a 2.5 GW off-shore wind power plant (WPP) project on the southwestern coast in 2011 [3].

WGs such as doubly-fed induction generators (DFIGs) and fully-rated converter based WGs, which have good controllability in terms of the active power and reactive power and so on, are commonly used. Their variable speed operation enables them to have a maximum power point tracking (MPPT) control scheme. However, this reduces the system inertia, and thus, a significant frequency deviation is inevitable when a large disturbance happens in the power system [4].

Wind generation frequency support schemes can be classified into two groups, i.e. inertial control and primary control. The former uses its kinetic energy that is stored in

† Corresponding author: Dept. of Electrical Engineering, WeGAT Research Center and Smart Grid Research Center, Chonbuk National University, Korea. (yckang@jbnu.ac.kr)
* Dept. of Electrical Engineering and WeGAT Research Center, Chonbuk National University, Korea. ({2jinshik, wannabeblack, love35021} @jbnu.ac.kr)
** Dept. of Electrical Engineering, Hongik University, Korea. (yhchun @hongik.ac.kr)
*** Korea Electrotechnology Research Institute, Korea. (sanghlee@keri. re.kr).
§ Dept. of Electrical Engineering, Yeungnam University, Korea. (doljk @ynu.ac.kr)
Received: April 9, 2013; Accepted: May 27, 2013

the rotor, whilst the latter uses the reserved power, which is de-loaded by the pitch control or rotor speed control. Many studies have been reported on the frequency support of DFIG-based wind generation [5-8]. Only an inertial control scheme was used in [5, 6], whilst [7, 8] used both inertial and primary control schemes.

To generate a power reference signal to release the power from the kinetic energy stored in the rotor of the DFIG, an auxiliary loop based on the rate of change of the frequency (ROCOF) was proposed in [5]. In addition, another loop based on the frequency deviation was added to the ROCOF loop in [6].

Frequency support schemes using both inertial and primary control were suggested [7, 8]. Only the frequency deviation loop was used in [7], whilst both the frequency deviation loop and the ROCOF loop were used in [8]. The schemes control the rotor speed for power de-loading.

On the other hand, the wind speed that arrives at the downstream WG is decreased after having passed through one WG, which is called the wake effect. Thus the rotor speeds are different from one another because the WGs are operating in MPPT mode. In other words, each WG has different kinetic energy available for the frequency support contribution. Therefore, the different gains for the inertial control of each WG depending on the rotor speed can give more contribution to the frequency support.

This paper proposes an algorithm that assigns the droop of each WG in a WPP based on the rotor speed for the virtual inertial control considering the wake effect. It assumes that every single WG has two auxiliary loops for the virtual inertial control, i.e. the frequency deviation and ROCOF loops. In this paper, to allow the WGs with high rotor speed to release more kinetic energy, the smaller droop of the WG, which is the gain of the frequency deviation loop, is assigned depending on the rotor speed of the WG. On the other hand, the ROCOF gain relies on the system and operating conditions, and careful attention should be paid to the determination of the gain. However, it is out of the scope of this paper, and thus the gains for the ROCOF loops of all of the WGs are set to be equal in this paper. The performance of the proposed algorithm is investigated through a model system, which consists of five SGs and a 75 MW WPP with fifteen DFIGs, using an EMTP-RV simulator under various conditions.

2. Rotor Speed-based Droop of a WG in a WPP for the Virtual Inertial Control

The goal of this paper is to release more kinetic energy to contribute more to the frequency support. On the other hand, each WG has different kinetic energy depending on the wind speed due to the wake effect. In this paper, it is assumed that a WG in a WPP has two auxiliary loops for the virtual inertial control, i.e. the frequency deviation loop and ROCOF loop. R and K are the gains of the frequency deviation and ROCOF loops, respectively. In addition, this paper assumes that all WGs are operating in MPPT control mode, and thus have no de-loaded power.

To release more kinetic energy, a smaller value of R is assigned to a WG with high rotor speed. However, the same value of K is assigned to all WGs for convenience, as mentioned in the Introduction.

2.1 Auxiliary loops of a WG for the virtual inertial control [6, 8]

Fig. 1 shows the two auxiliary loops for the virtual inertial control implemented in each DFIG in a WPP. The top loop is based on the ROCOF and the bottom one is based on the frequency deviation.

The active power reference for a DFIG, P_{ref}, is composed of three terms, i.e. P_{MPPT} for the MPPT, ΔP, which is derived from the frequency deviation loop, and ΔP_{in} from the ROCOF loop.

In the bottom loop of Fig. 1, the droop, R, is used to obtain ΔP from the frequency deviation. ΔP can be derived from the droop characteristics.

$$\Delta P = -\frac{1}{R}(f_{sys} - f_{nom}) \tag{1}$$

When the system frequency is smaller than the nominal frequency, ΔP becomes positive, and this makes the WG to increase the active power.

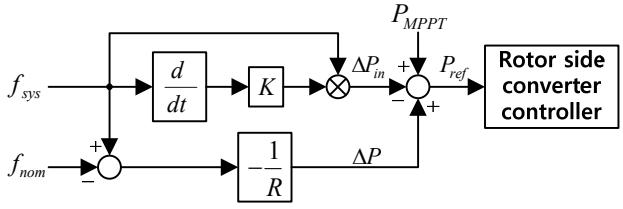

f_{sys}: system frequency — f_{nom}: nominal frequency
K: gain of the ROCOF loop — R: droop gain
P_{MPPT}: reference for MPPT — ΔP_{in}: reference from top loop
ΔP: reference from bottom loop — P_{ref}: reference for the RSC

Fig. 1. Virtual inertial control loops of a WG

2.2 Wake effect

In a WPP, which consists of multiple WGs, a WG located upstream in the wind direction decreases the wind speed at the WG locations on its downstream side, which is called the wake effect [9]. Hence, the rotor speeds of the WGs downstream are different from those of the WGs upstream, because the WGs are assumed to be operating in MPPT control mode.

2.3 Assignment of the droop for a WG based on the rotor speed

In this paper, to release more kinetic energy, different values of R are assigned to all WGs, depending on their rotor speeds.

Rearranging (1) yields

$$\frac{\Delta P}{f_{sys}-f_{nom}}=-\frac{1}{R} \tag{2}$$

The unit of the left hand side is W·sec, which is the same as that of the energy. Therefore, the kinetic energy to be released from WG_i, ΔE_i, can be represented by:

$$\Delta E_i \propto \frac{\Delta P}{f_{sys}-f_{nom}}=-\frac{1}{R_i}, \quad for\, i=1,\cdots,m \tag{3}$$

where R_i is the droop of WG_i and m is the number of WGs in a WPP. Eq. (3) indicates that ΔE_i is inversely proportional to R_i. In other words, the product of ΔE_i and R_i is constant.

ΔE_i can be expressed by:

$$\Delta E_i=\frac{1}{2}J(\omega_i^2-\omega_{\min}^2), \quad for\, i=1,\cdots,m \tag{4}$$

where ω_i and $\omega_{\min}$ are the operating rotor speed and the minimum rotor speed, respectively. In this paper, since the WG is in MPPT control mode, ω_i is set to be a constant prior to the disturbance, and $\omega_{\min}$ is set to 0.7pu

$$\Delta E_i R_i=\Delta E_{\max} R_{\min}, \quad for\, i=1,\cdots,m \tag{5}$$

where $\Delta E_{\max}$ and $R_{\min}$ are the maximum energy to be released and the minimum droop, respectively. $\Delta E_{\max}$ in (5) can be obtained by inserting $\omega_{\max}$, which is set to 1.25 pu, into (4).

In (5), $R_{\min}$ can be determined in various ways. In this paper, $R_{\min}$ is determined so that the rotor speed of the WG rotating at the smallest rotor speed in a WPP should not drop below 0.7 pu, which is the minimum operating rotor speed, after the inertial control.

Therefore, R_i can be obtained by:

$$R_i=R_{\min}\times\frac{\Delta E_{\max}}{\Delta E_i} \tag{6}$$

3. Model system

To investigate the performance of the proposed WPP virtual inertial control algorithm, a model system as shown in Fig. 2 is chosen. The system consists of five SGs, one DFIG-based WPP, and a load of 600 MW and 9 MVAr. The detailed information on the generators will be described in the following subsections.

3.1 Synchronous generators

Five SGs (two 200 MVA SGs, two 150 MVA SGs, and one 100 MVA SG) are interconnected in the model system.

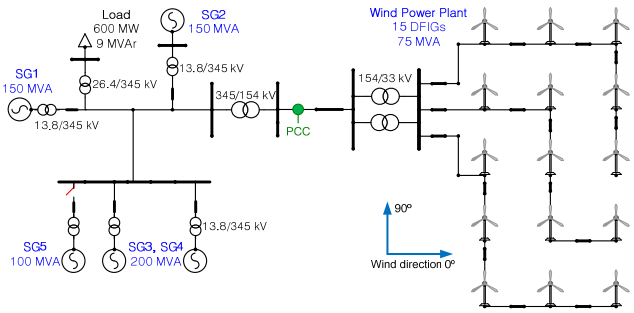

Fig. 2. Model system configuration

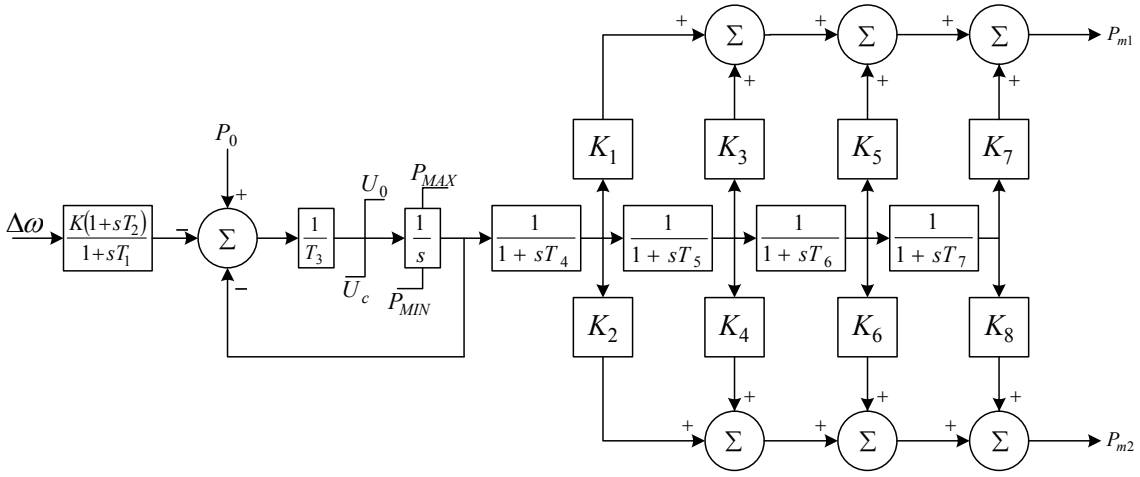

Fig. 3. IEEEG1 steam governor model

Table 1. Coefficients of the IEEEG1 model

K	K_1	K_2	K_3	K_4	K_5	K_6	K_7	K_8	P_{MAX}
20	0.3	0	0.4	0	0.3	0	0	0	1
T_1	T_2	T_3	T_4	T_5	T_6	T_7	U_o	U_c	P_{MIN}
0.1	0	0.25	0.3	10	0.4	0	0.3	-0.5	0.33

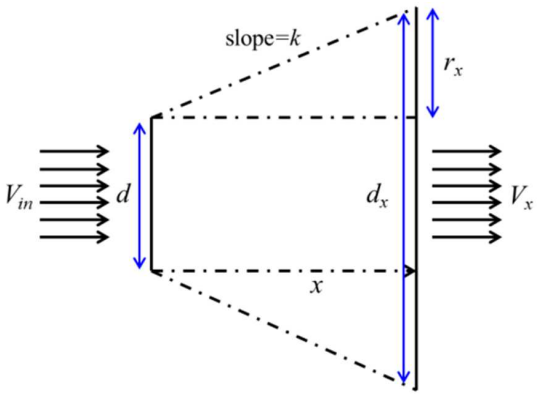

V_x: wind speed at *distance x* V_{in}: *incoming wind speed*
C_t: *thrust coefficient* d: *wind turbine diameter*
$d_x = d + 2r_x = d + 2$ k: wake decay constant

Fig. 4. Jensen's wake model

For convenience, it is assumed that all of the generators in the system are steam turbine generators, and their steam turbine governor model is shown in Fig. 3. In addition, Table 1 shows the coefficients of the governor. The droop on all steam governors is set to 5%.

3.2 WPP configuration

In the WPP configuration shown in Fig. 2, which is a tentative configuration for the first stage of the Korea's 2.5 GW off-shore WPP project, three feeders are connected to the collector bus, and five 5MW DFIGs are connected to each feeder. The distance between the two WGs is 1,080 m, which is 9*D*, where *D* is the wind turbine diameter. In addition, the collector bus is connected to the intertie through the two 60 MVA substation transformers, and a 22 km submarine intertie cable connects the transformers to the on-shore grid.

In this paper, Jensen's model is used as a wake model [10] as shown in Fig. 4. In Jensen's model, the relationship between the wind speeds of the two WGs can be represented by:

$$V_x = V_{in}\left\{1-(1-\sqrt{1-C_t})\left(\frac{d}{d_{xi}}\right)^2\right\} \quad (7)$$

Fig. 5 shows the characteristics of a DFIG. The operational rotor speed range of the DFIG is 0.7 pu-1.25 pu. In the power curve of the DFIG in Fig. 5(b), the cut-in, rated, and cut-out wind speeds are 4, 10.5, and 25 m/s,

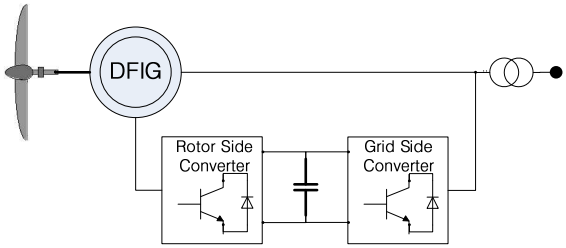

(a) DFIG configuration

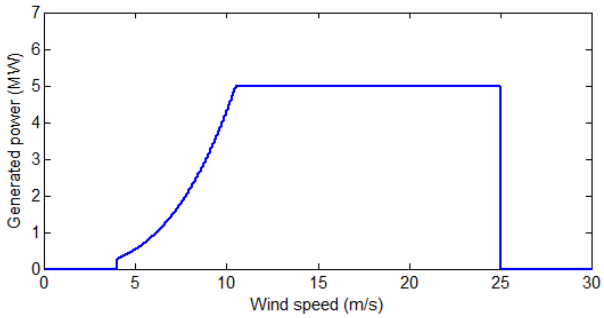

(b) Power curve of a DFIG

Fig. 5. Characteristics of the DFIG used

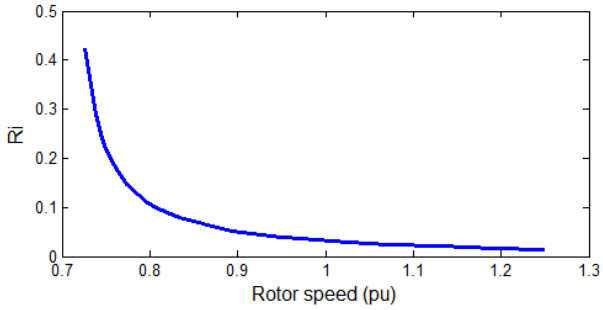

Fig. 6. Assigned droop of the WG (R_{min} = 0.015)

respectively. For the MPPT control, the control method in [11] is used in this paper, and the reference for the total output of the DFIG is set to be $k_g\omega_r^3$.

As shown in Fig. 6, the relation between the droop of the WG and the rotor speed is obtained from (6), where R_{min} is set to be 0.015. On the other hand, the ROCOF gain K is set to be 10 in both the conventional and proposed algorithms.

4. Case studies

In the model system, as a disturbance, SG5, which supplies 70 MW to the load, is assumed to be tripped out at t = 40 s. Three cases are tested with wind directions of 0° and 90°, and wind speeds of 8 m/s and 10 m/s. Due to the wake effect, the input wind speeds of the WGs in the WPP are different from one another, and Table 2 shows the wind speeds of the WGs for the three cases.

Table 2. Wind speeds of WGs for three cases considering the wake effect

Case 1 (m/s)		
8.0	6.8	6.2
8.0	6.8	6.2
8.0	6.8	6.2
8.0	6.8	6.2
8.0	6.8	6.2

Case 2 (m/s)		
10.0	8.6	8.0
10.0	8.6	8.0
10.0	8.6	8.0
10.0	8.6	8.0
10.0	8.6	8.0

Case 3 (m/s)		
7.4	7.4	7.4
7.6	7.6	7.6
8.0	8.0	8.0
8.6	8.6	8.6
10.0	10.0	10.0

In cases 1-3, the performance of the proposed algorithm is compared with that of a conventional algorithm [6]. Figs. 7(a)-9(a) show the system frequencies before and after the disturbance, and Figs. 7(b)-9(b) indicate the active power of the WPP. In these figures, the bold, thin, and dotted lines represent the results for the proposed algorithm, the conventional algorithm, and no inertial control, respectively.

4.1 Case 1: *wind speed of 8 m/s, wind direction of 0°*

Fig. 7 shows the results for case 1. As shown in Fig. 7(b), the conventional and proposed algorithms start to release the kinetic energy based on the frequency deviation and the ROCOF. The maximum released power values for the conventional and proposed algorithms are 5.8 MW and 9.0 MW, respectively. The proposed algorithm assigns different droops, i.e. 0.038 for the WGs at the 1st column, 0.100 for the 2nd column, and 0.281 for the 3rd column, whilst the conventional algorithm uses the same droop of 0.281 for all of the WGs. We can see that the droops for the proposed algorithm are less than those of the conventional algorithm. Thus, the proposed algorithm could release more kinetic energy than the conventional algorithm. Thus, after the disturbance, the frequency nadir for the proposed algorithm is the highest, i.e. 59.44 Hz.

From Figs. 7(c) and 7(d), the rotor speed reductions for the proposed algorithm are 0.09 pu for the 1st column, 0.04 pu for the 2nd column, and 0.02 pu for the 3rd column. On the other hand, the rotor speed reductions for the conventional algorithm are 0.01 pu for the 1st column, 0.02 pu for the 2nd column, and 0.02 pu for the 3rd column. For the conventional algorithm, the rotor speed reduction of the WG with small rotor speed is larger than that with high

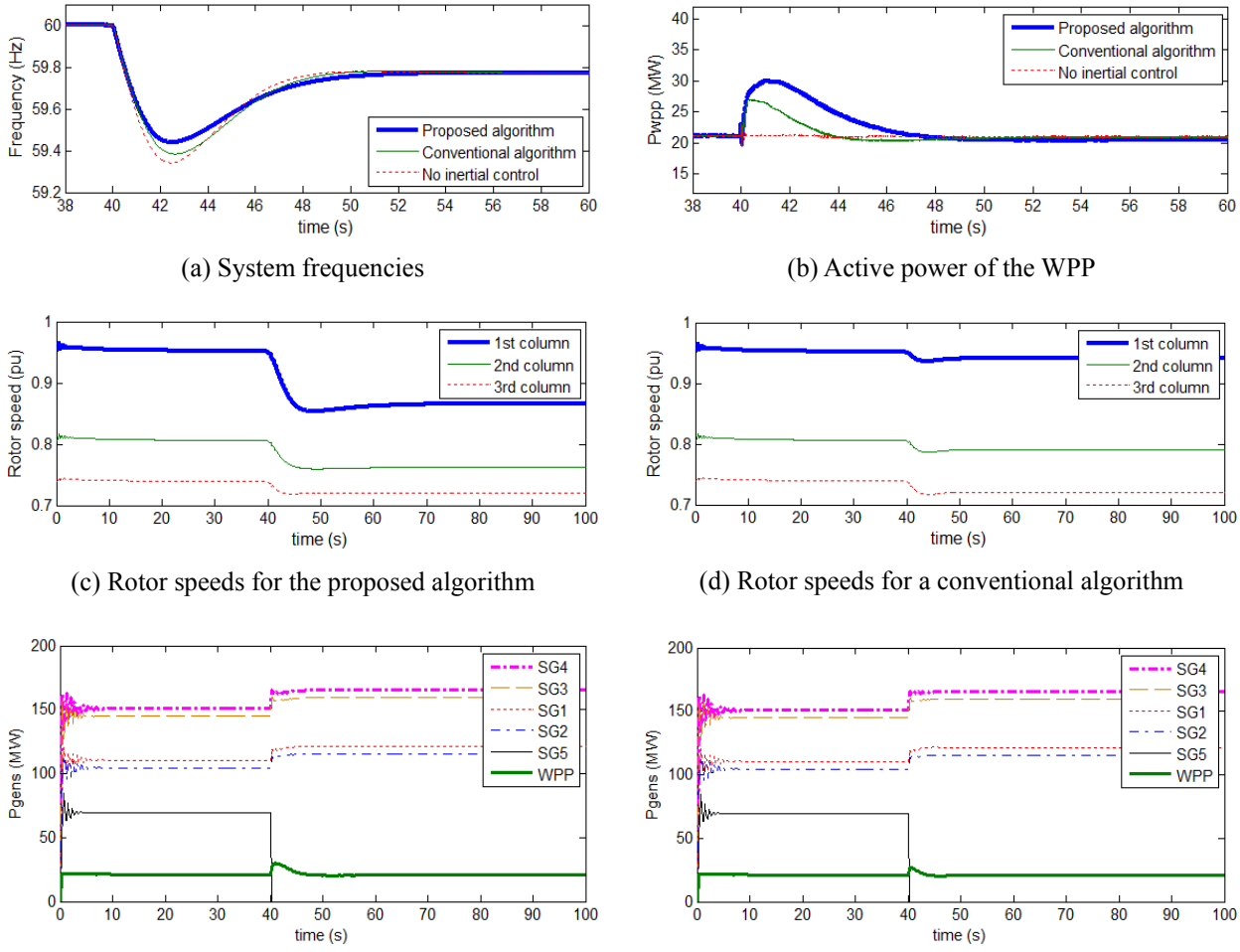

(a) System frequencies

(b) Active power of the WPP

(c) Rotor speeds for the proposed algorithm

(d) Rotor speeds for a conventional algorithm

(e) Active power of generators for the proposed algorithm

(f) Active power of generators for a conventional algorithm

Fig. 7. Results for case 1

rotor speed. This might increase the probability that the WG with small rotor speed is over-decelerated below the operating range. Thus, for the conventional algorithm, careful attention should be paid to the selection of the droop so that no WGs will be over-decelerated.

As shown in Figs. 7(e) and 7(f), the increase of the SG output for the proposed algorithm is smaller than that for the conventional algorithm, because more energy with the proposed algorithm are released than with the conventional algorithm. Therefore, the frequency drop for the proposed algorithm is smaller than that of the conventional algorithm.

4.2 Case 2: *wind speed of 10 m/s, wind direction of 0°*

Fig. 8 shows the results for case 2, which is identical to case 1 except for the wind speed. In this case, the maximum released power for the conventional and proposed algorithms are 13.5 MW and 18.0 MW, respectively. The droops assigned for the proposed algorithm are 0.017 for the WGs at the 1st column, 0.029 for the 2nd column, and 0.039 for the 3rd column, whilst the conventional algorithm uses the same droop of 0.039 for all of the WGs. In this case, the droops of the WGs are smaller than those in case 1 because of the high wind speed. After the disturbance, the frequency nadir for the proposed algorithm is the highest, i.e. 59.55 Hz.

From Figs. 8(c) and 8(d), the rotor speed reductions for the proposed algorithm are 0.13 pu for the 1st column, 0.10 pu for the 2nd column, and 0.09 pu for the 3rd column. On the other hand, the rotor speed reductions for the conventional algorithm are 0.05 pu for the 1st column, 0.07 pu for the 2nd column, and 0.09 pu for the 3rd column. The

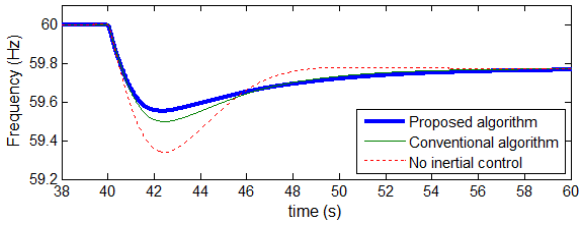

(a) System frequencies

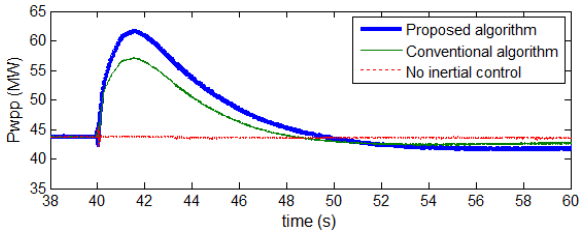

(b) Active power of the WPP

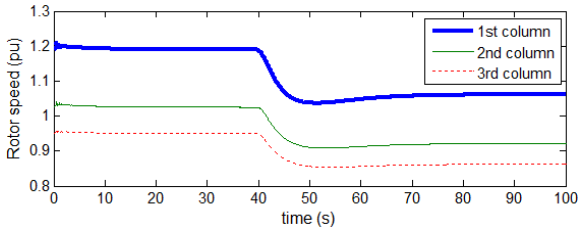

(c) Rotor speeds for the proposed algorithm

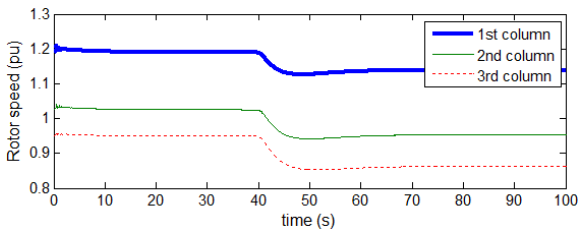

(d) Rotor speeds for a conventional algorithm

Fig. 8. Results for case 2

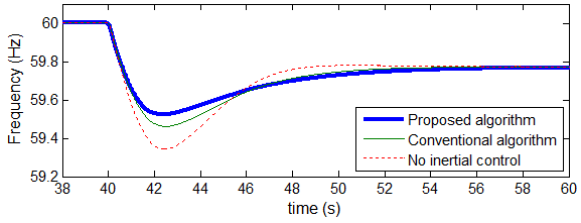

(a) System frequencies

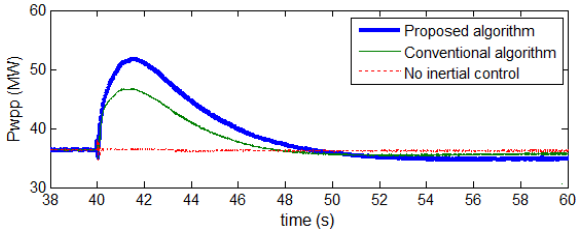

(b) Active power of the WPP

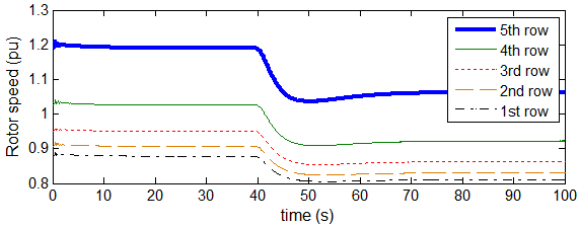

(c) Rotor speeds for the proposed algorithm

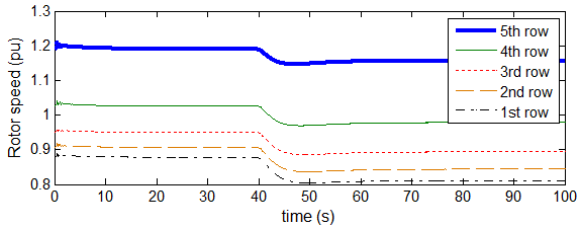

(d) Rotor speeds for a conventional algorithm

Fig. 9. Results for case 3

reduction of the rotor speed in case 2 is larger than that of case 1, and thus a WPP for the high wind speed can give more contribution to the frequency support.

4.3 Case 3: *wind speed of 10 m/s, wind direction of 90°*

Fig. 9 shows the results for case 3, which is identical to case 2 except for the wind direction. In this case, the maximum released power for the proposed algorithm is 15.6 MW, which is smaller than for case 2. This is because the wake effect in this case is more severe than in case 2 due to the 90° wind direction. In this case, the droop for the proposed algorithm ranges from 0.017 to 0.057. For the conventional algorithm, the droop is set to be 0.057 for all of the WGs. After the disturbance, the frequency nadir for the proposed algorithm is 59.52 Hz, which is smaller than that of case 2.

The results clearly indicate that a WPP gives different contributions to the frequency support depending on the degree of the wake effect.

5. Conclusion

This paper proposes an algorithm for assigning the droop of each WG in a WPP based on the rotor speed for the virtual inertial control considering the wake effect. To release more kinetic energy, the smaller droop is assigned to the WG with high rotor speed.

The results show that the proposed algorithm can give more contribution to the frequency support than the conventional algorithm because it can release more energy during the disturbance. The contribution depends on the kinetic energy that a WPP contains. The proposed algorithm might help maximize the contribution of the WPP for the frequency support.

It is seen that the WPP output in the steady state after the disturbance is smaller than that before the disturbance, because the system frequency is not completely recovered to the nominal value. However, it can be recovered to the MPPT value after AGC action from the grid control center.

Acknowledgements

This work was supported by the National Research Foundation of Korea (NRF) grant funded by the Korea government (MSIP) (2012-0009146).

References

[1] T. Ackermann, *Wind Power in Power System*, 2nd Edition, England, John Wiley & Sons, Ltd, 2012.

[2] *Global wind energy outlook 2010*, Global Wind Energy Council, Oct. 2010.

[3] *Global Wind Energy Report: Annual market update 2011*, Global Wind Energy Council, Mar. 2012.

[4] O. Anaya-lara, N. Jenkins, J. Ekanayake, P. Cartwright, and M. Hughes, *Wind Energy Generation Modeling and Control*, John Wiley & Sons, Ltd, 2009.

[5] J. Ekanayake and N. Jenkins, "Comparison of the response of doubly fed and fixed-speed induction generator wind turbines to changes in network frequency," *IEEE Transaction on Energy con-version*, Vol. 19, No. 4, 2004, pp. 800-802.

[6] J. Morren, S. Haan, W. L. Kling, and J. A. Ferreira, "Wind turbines emulating inertia and supporting primary frequency control," *IEEE Transaction on Power systems*, Vol. 21, No. 1, 2006, pp. 433-434.

[7] R. G. Almeida and J. A. P. Lopes, "Participation of doubly red induction wind generator in system frequency regulation," *IEEE Transaction on Power systems*, Vol. 22, No. 3, 2007, pp. 944-950.

[8] Z. S. Zhang, Y. Z. Sun, J. Lin, and G. J. Li, "Coordinated frequency regulation by doubly fed induction generator-based wind power plants," *IET Renew. Power Gener.*, Vol. 6, No. 1, 2012, pp. 38-47.

[9] F. Koch, M. Gresch, F. Shewarega, I. Erlich, and U. Bachmann "Consideration of wind farm wake effect in power system dynamic simulation," *Power Tech*, Russia, June 27-30, 2005.

[10] N. O. Jensen, "A Note on Wind Generation lnteraction," RISO, Nov 1983.

[11] B. Shen, B. Mwinyiwiwa, Y. Zhang, and B. Ooi, "Sensorless Maximum Power Point Tracking of Wind by DFIG Using Rotor Position Phase Lock Loop," *IEEE Transaction on Power Electronics*, Vol. 24, No. 4, 2009, pp. 942-951.

Jinsik Lee He received the B. S. degree from Chonbuk National University, Korea in 2011. He is currently pursuing an M. S. degree at Chonbuk National University. He is also an assistant researcher at the Wind energy Grid-Adaptive Technology (WeGAT) Research Center supported by the Ministry of Education, Science, and Technology, Korea. His research interest is control systems for wind power plants.

Jinho Kim He received the B. S. degree from Chonbuk National University, Korea in 2013. He is currently pursuing an M. S. degree at Chonbuk National University. He is also an assistant re-searcher at the WeGAT Research Center. His research interest is the development of control and protection methods for wind power plants.

Yeon-Hee Kim He received his B.S. and M.S. degrees from Chonbuk National University, Korea, in 2006 and 2008, respectively. He is currently pursuing a Ph.D. degree from Chonbuk National University, Korea. He is also an assistant researcher at the WeGAT Research Center. His research interest is the development of new control/protection systems for wind power plants and power systems using digital signal processing techniques.

Yeong–Han Chun He received his B.S. and M.S. degrees from Seoul National University, Korea, in 1983 and 1985, respectively, and his Ph.D. degree from Tokyo University, Japan, in 1997. He was with the Korea Electro-technology Research Institute (KERI) from 1985 to 2002, and joined Hongik University, where he is currently a Professor of Electrical Engineering. His research interests are power system control and stability.

Sang Ho Lee He received his B.S., M.S., and Ph.D. degrees from Seoul National University, Korea, in 1995, 1997, and 2003, respectively. He has been with Korea Electrotechnology Research Institute (KERI), Korea, since 2003. He is currently a senior researcher at KERI, Korea. His research interests are the development of an energy management system for power system and wind farms, and optimal operating schemes for the smart grid.

Jul-Ki Seok He received the B.S., M.S., and Ph.D. degrees from Seoul National University, Seoul, Korea, in 1992, 1994, and 1998, respectively, all in electrical engineering. From 1998 to 2001, he was a Senior Engineer with the Production Engineering Center, Samsung Electronics, Suwon, Korea. Since 2001, he has been a member of the faculty of the School of Electrical Engineering, Yeungnam University, Gyeongsan, Korea, where he is currently a Professor. His specific research areas are motor drives, power converter control of offshore wind farms, and nonlinear system identification related to the power electronics field.

Yong Cheol Kang He received his B.S., M.S., and Ph.D. degrees from Seoul National University, Korea, in 1991, 1993, and 1997, respectively. He has been with Chonbuk National University, Korea, since 1999. He is currently a professor at Chonbuk National University, Korea, and the director of the WeGAT Research Center. He is also with the Smart Grid Research Center at Chonbuk National University. His research interests are the development of new protection and control systems for wind power plants and the enhancement of wind energy penetration levels by keeping the capacity factor of wind generators high.